NASA TECHNICAL NOTE

NASA TN D-6102

AN IMPROVED ANALYTICAL TREATMENT OF THE DENTING OF THIN SHEETS BY HAIL

by Robert G. Thomson and Robert J. Hayduk

Langley Research Center
Hampton, Va. 23365

NATIONAL AERONAUTICS AND SPACE ADMINISTRATION • WASHINGTON, D. C. • JANUARY 1971

1. Report No.	2. Government Accession No.	3. Recipient's Catalog No.
NASA TN D-6102		

4. Title and Subtitle	5. Report Date
AN IMPROVED ANALYTICAL TREATMENT OF THE DENTING OF THIN SHEETS BY HAIL	January 1971
	6. Performing Organization Code

7. Author(s)	8. Performing Organization Report No.
Robert G. Thomson and Robert J. Hayduk	L-7343
	10. Work Unit No.
9. Performing Organization Name and Address	126-61-10-01
NASA Langley Research Center Hampton, Va. 23365	11. Contract or Grant No.
	13. Type of Report and Period Covered
12. Sponsoring Agency Name and Address	Technical Note
National Aeronautics and Space Administration Washington, D.C. 20546	14. Sponsoring Agency Code

15. Supplementary Notes

16. Abstract

Severe structural damage, such as surface erosion, dents, perforations, and tears, can occur when high-speed aircraft collide with hailstones. In this paper the denting of aircraft skin by hail is mathematically analyzed and the results are compared with experimental data. The denting process is modeled mathematically by assuming that a crushable, spherical hailstone impacts normal to a flat sheet. The resultant dent depth and shape are determined by utilizing an existing computer program which considers both bending and membrane action and elastic and plastic material behavior. The results of this analysis are compared with experimental data from the British Royal Aircraft Establishment and with a previous analysis which considered bending only. The improved analytical treatment of the denting process agrees well with the experimental data and shows that membrane forces must be considered when sheet deflections are large.

17. Key Words (Suggested by Author(s))	18. Distribution Statement
Hailstones Denting Plastic Flat sheets Impact	Unclassified – Unlimited

19. Security Classif. (of this report)	20. Security Classif. (of this page)	21. No. of Pages	22. Price*
Unclassified	Unclassified	36	$3.00

*For sale by the National Technical Information Service, Springfield, Virginia 22151

AN IMPROVED ANALYTICAL TREATMENT OF THE DENTING OF THIN SHEETS BY HAIL

By Robert G. Thomson and Robert J. Hayduk
Langley Research Center

SUMMARY

Severe structural damage, such as surface erosion, dents, perforations, and tears, can occur when high-speed aircraft collide with hailstones. In this paper the denting of aircraft skin by hail is mathematically analyzed and the results are compared with experimental data. The denting process is modeled mathematically by assuming that a crushable, spherical hailstone impacts normal to a flat sheet. The resultant dent depth and shape are determined by utilizing an existing computer program which considers both bending and membrane action and elastic and plastic material behavior. The results of this analysis are compared with experimental data from the British Royal Aircraft Establishment and with a previous analysis which considered bending only. The improved analytical treatment of the denting process agrees well with the experimental data and shows that membrane forces must be considered when sheet deflections are large.

INTRODUCTION

Severe structural damage can occur when high-speed aircraft collide with hailstones. Large hailstones erode surfaces, cause dents, and perforate and tear sheet-metal skins. References 1, 2, and 3 show photographic evidence of such damage to leading edges, empennages, and forward sections as well as photographs of shattered windshields. Methods of predicting hail damage to aircraft surfaces are needed to determine how aircraft should be designed to survive an accidental encounter with hail.

The skin deformations resulting from hail impact usually are plastic near the point of impact and elastic in the surrounding area. Reference 4 was a first attempt at predicting the denting characteristics of hail on thin sheets. In that reference the permanent deformations were predicted by an approximate elastic-plastic analysis. Classical thin-plate bending theory was used to circumvent the difficulties of a large-deformation analysis which would include both bending and membrane effects. However, recent hail-impact data from the British Royal Aircraft Establishment (R.A.E.) indicate that membrane forces must be included. (See ref. 5.) The results of the bending analysis of reference 4 deviate from these experimental data when sheet deflections are comparable

with sheet thickness or larger. A similar conclusion was reached by A. L. Florence in reference 6, which presents the results of an experimental investigation of circular plates subjected to uniformly distributed impulses. Florence compared the experimentally obtained permanent deformations with those predicted by rigid-plastic bending theory and concluded that a "full treatment of the problem taking account of the membrane action is certainly required."

The evidence indicates that large-deformation theory is required to analyze the hail-impact problem; therefore, this paper presents an improved analytical treatment which includes the effects of membrane action. The solution was accomplished by adapting the DEPROSS 3 computer program to the hail-impact problem. DEPROSS 3 was developed at Massachusetts Institute of Technology by E. A. Witmer, H. A. Balmer, J. W. Leech, T. H. H. Pian, and W. Herrmann (see refs. 7, 8, and 9) to analyze the dynamic elastic-plastic response of impulsively loaded simple structures. With minor modifications in the initial velocity input section and the addition of the hailstone mass to the mass of the plate, the program was employed to predict the size of the dents caused by hail.

A discussion of the modifications made to DEPROSS 3, the final permanent deformations obtained, and comparisons with the bending solution of reference 4 and the R.A.E. experimental data are presented herein.

The authors gratefully acknowledge the assistance offered them by the British Royal Aircraft Establishment. Through personal communication with Ian I. McNaughton of the R.A.E., the authors received supplementary data on hail impact with aircraft. These supplementary data included unpublished results for 1.27- and 1.91-cm- (0.5- and 0.75-inch-) diameter hail-impact for flat sheets.

SYMBOLS

The units used for the physical quantities defined in this paper are given both in the International System of Units (SI) and in the U.S. Customary Units. (See ref. 10.) Appendix A presents factors relating these two systems of units. The measurements and calculations were made in the U.S. Customary Units.

A radius of crushed hailstone, aK_2

a radius of hailstone

b radius of central plastic region, where $M_r = 0$

$c = \sqrt{E/\rho_s}$

D flexural rigidity of sheet, $Eh^3/12(1 - \nu^2)$

E elastic modulus of sheet material in tension and compression

g_o hailstone impact velocity

h thickness of sheet

i integer

$J_n(z)$ Bessel function of the first kind, where n is the order of the Bessel function

K_1 factor which adjusts the height of the crushed hailstone,

$$K_1 = \frac{2}{\left[K_2^3 - \left(K_2^2 - 1\right)^{1.5}\right]K_2^2}$$

K_2 factor representing the instantaneous spread of the base of the hailstone (i.e., a factor of 1.5 or 2.0)

$k = \frac{2a^2}{ch}\sqrt{3(1 - \nu^2)}$

M_o yield-moment resultant, $\sigma_o(h/2)^2$; maximum bending moment that sheet can sustain

M_r, M_θ radial and circumferential bending-moment resultants

m mass distribution

p Hankel transform parameter

R radius of finite sheet

r,z radial and transverse coordinates (see fig. 1)

ΔS_i distance between mass stations, where $i = 1, 2, \ldots$

t time

t^* time of cessation of all sheet motion after impact

$$V_o = \frac{\frac{K_1 A}{h}\frac{\rho_p}{\rho_s} g_o}{1 + \frac{K_1 A}{h}\frac{\rho_p}{\rho_s}\psi} \quad \left(K_1 = 2 \text{ for bending-only analysis (see ref. 4)}\right)$$

w sheet deflection in transverse direction (z-direction)

δ permanent center deflection, $w(0,t^*)$

$\eta = r/A$

μ mass per unit area of sheet, $\rho_s h_s$

ν Poisson's ratio

$\xi = \frac{b}{A}$

ρ mass density

σ_o yield stress in simple tension or compression (assumed to be identical in magnitude)

$\tau = t/k$

ψ momentum constant, set equal to 0.70 (see ref. 4)

Subscripts:

p projectile

s sheet

A dot over a symbol indicates partial differentiation with respect to time t.

COMPUTER ANALYSIS

Program Description

The DEPROSS 3 computer program used in this analysis is described in detail in references 7, 8, and 9. A brief description of the program will be included in this section, but the emphasis will be on the minor modifications made to the program and the results obtained from it. The modifications adapted the program to the specific problem of hail impact on thin sheets.

DEPROSS 3 is a numerical computer program capable of predicting the dynamic, axisymmetric response of shells, plates, rings, and beams to impulsive or blast loads. Material behavior can be elastic, elastic-perfectly-plastic, elastic-strain-hardening, or elastic-strain-hardening with strain-rate sensitivity. The elastic-strain-hardening material behavior was chosen to represent the response of the thin sheets to hail impact. A bilinear stress-strain relationship was adopted in which the target material was assumed to behave elastically up to the yield stress at 0.2-percent offset and then to experience linear strain-hardening between the yield stress and the ultimate stress. The coordinates of the bilinear stress-strain curve used in the computer program are listed in table I.

The model which represents the simple structure consists of concentrated masses connected by massless links. The links can extend or contract axially but are infinitely rigid in bending; all bending action takes place at the mass points. External forces are applied at these mass points; internal forces and moments are transmitted between the masses by the links. The dynamic equilibrium equations are solved numerically in finite-difference form for each mass point at successive time increments. The increments in the forces and moments at each mass location are determined by representing each mass station as consisting of a number of discrete layers of material. Each layer carries normal stresses and is separated from an adjacent layer by a material that has infinite shear rigidity and does not carry normal stresses. The axial force and bending moment at each mass location can then be determined from the normal stresses in the various layers. The strain in each layer is determined by adding the midplane strain and the bending strain due to curvature, that is, plane sections remain plane during deformation. Rotary inertia and transverse shear deformations are assumed to be negligible.

Determination of the Mass Distribution for the Program

The flat surface of a wing panel is represented in the DEPROSS 3 program as a flat, circular, clamped sheet of uniform thickness. The radius of the circular sheet is taken to be large enough so that the effects of the clamped boundary on the central deflection of the sheet are negligible. In reference 5, it was observed that "the indentation base shape

[of the hailstone] is formed very rapidly and is maintained throughout the impact phase being progressively driven deeper through the plate. In the case of 1 inch hail impacting on L73 material [2014-T6, U.S. equivalent], the base shape is that of a 2 inch diameter sphere and on L72 material [2014-T4, U.S. equivalent] it is a 1.5 inch diameter sphere." Two constants $(K_1$ and $K_2)$ were introduced into the analysis to account for this experimental observation. The constant K_2 in the present analysis represents the instantaneous spread of the base of the hailstone (i.e., a factor of 1.5 or 2.0). The height of the crushed hailstone was adjusted by the factor K_1

$$K_1 = \frac{2}{\left[K_2^3 - \left(K_2^2 - 1\right)^{1.5}\right] K_2^2} \tag{1}$$

to yield the same mass as the original uncrushed hailstone.

The mass distribution of this crushed hailstone and sheet is shown in figure 1(a). The radial coordinate r of the sheet is nondimensionalized by dividing by the base radius of the crushed hailstone, $A = aK_2$,

$$\eta = \frac{r}{A} \tag{2}$$

The sheet material was concentrated in 32 mass stations equally spaced along the radius, as shown in figure 1(b). This number of mass stations adequately represented the dynamic response of the sheet. (See ref. 8.) The first and last mass stations were one-half of a space away from the origin and boundary, respectively. The mass of the crushed hailstone was also distributed among the mass stations. The mass stations were chosen so that an integer number of mass points were beneath the hailstone. The mass distribution of the crushed hailstone is given by

$$m_p(\eta) = K_1 A \sqrt{1 - \eta^2}\rho_p \qquad (0 \leqq \eta \leqq 1) \tag{3}$$

This exact mass distribution is shown in figure 1(b) along with the stepwise approximation. The additional mass contributed by the hailstone at each station was calculated by taking the mass distribution as uniform between stations and equal to the value obtained from equation (3) for the η's corresponding to the mass stations. The mass at the last station adjacent to the periphery of the hailstone was adjusted so that the total mass included in the stepwise DEPROSS 3 distribution was equal to the total mass of the hailstone.

In the calculations, the number of mass stations beneath the projectile varied with hail size and target material. When the hail diameters were modified by the K_2 factor of 1.5 and 2.0 for L72 and L73, respectively, there were 6 or 8 mass stations beneath the 2.54-cm- (1-inch-) diameter hail, 4 or 6 beneath the 1.91-cm- (0.75-inch-) diameter hail, and 3 or 4 beneath the 1.27-cm- (0.50-inch-) diameter hail. For the 1.91-cm- (0.75-inch-) diameter hail and L72 target material, the plate radius was increased from 10.2 to 11.4 cm (4 to 4.5 inches) so that an integer number of mass stations was completely covered by the hailstone. An integer number of mass stations ensured a smooth velocity distribution. The details of the programing are given in appendix B, statement numbers 8 through 104. The computer program printed the displacements of the mass stations every 0.06 μs.

Determination of the Initial Velocity Distribution for the Program

The initial velocity distribution of the sheet and crushed hailstone was determined by assuming that the momentum exchange upon impact was instantaneous and axisymmetric. The momentum balance for a completely inelastic impact is

$$2\pi A^2 \eta \, d\eta \left[m_p(\eta) + m_s(\eta)\right] \dot{w}(\eta,0) = m_p(\eta) g_o 2\pi A^2 \eta \, d\eta \tag{4a}$$

or

$$\left[2\pi A^2 \eta \, d\eta \left(K_1 A \sqrt{1 - \eta^2}\right) \rho_p + 2\pi A^2 \eta \, d\eta \, h \rho_s\right] \dot{w}(\eta,0) = 2\pi A^2 \eta \, d\eta \left(K_1 A \sqrt{1 - \eta^2}\right) \rho_p q_o \tag{4b}$$

Solution of equation (4b) for the initial velocity distribution gives

$$\dot{w}(\eta,0) = \frac{\frac{K_1 A}{h} \frac{\rho_p}{\rho_s} g_o \sqrt{1 - \eta^2}}{1 + \frac{K_1 A}{h} \frac{\rho_p}{\rho_s} \sqrt{1 - \eta^2}} \qquad (0 \leqq \eta \leqq 1) \tag{5a}$$

$$\dot{w}(\eta,0) = 0 \qquad (\eta \geqq 1) \tag{5b}$$

The initial velocity distribution (eqs. (5)) for the combined mass of hailstone and sheet is illustrated in figure 1(c). The initial velocity imparted to each mass station was calculated from equations (5) using the η's corresponding to the stations except for the last mass station adjacent to the outer periphery of the hailstone. The velocity of this last mass station was adjusted so that the integrated, stepwise, initial velocity distribution

(see fig. 1(b)) was the same as the integrated, exact velocity distribution, equations (5). The program listing for the initial velocity distribution is given in appendix B (statement numbers 50 through 85).

EXPERIMENTAL DATA FROM BRITISH ROYAL AIRCRAFT ESTABLISHMENT

The R.A.E. has conducted extensive hailstone impact tests in order to obtain basic data on the hail-impact resistance of aircraft. The results of an experimental program using flat aluminum sheets as targets and 2.54-cm- (1-inch-) diameter hail are presented in reference 5. Additional data for other hailstone sizes were personally communicated to the authors. These supplementary R.A.E. data were for 1.27-cm- (0.50-inch-) diameter and 1.91-cm- (0.75-inch-) diameter hail. The target sheets were made from two different British aluminum alloys, designated L72 (2014-T4, U.S. equivalent) and L73 (2014-T6, U.S. equivalent). The mechanical properties of L72 and L73 are listed in table I. The sheets were 30.5 cm (12 inches) square and were bolted to a frame leaving a 20-cm- (8-inch-) square, unsupported area in the center. The sheet thicknesses were 0.071 cm (0.028 inch), 0.091 cm (0.036 inch), 0.122 cm (0.048 inch), and 0.163 cm (0.064 inch).

RESULTS AND DISCUSSION

The modified DEPROSS 3 program was used to calculate the permanent deformations of thin, flat sheets impacted by hailstones of various sizes. The sheet thicknesses and hailstone sizes corresponded to thicknesses and sizes used by the R.A.E. in its experimental studies. Since DEPROSS 3 handles only axisymmetric problems, the square experimental targets were idealized as 10.2-cm- (4-inch-) radius clamped circular plates. The difference in the shape between the experimental and idealized targets seems to be unimportant inasmuch as the permanent depth of the dent was established by calculations before the disturbance reached the boundary of the target. Additional calculations were made using the classical bending approach of reference 4 for comparison purposes. The following sections will discuss these calculations and comparisons.

Sheet Displacements

The computed shapes of the sheet at various times (24, 102, 204, and 420 μs) are shown to scale in figure 2 for two impact conditions. After impact the disturbance travels radially out to the boundaries as the plate deflects. The deflection of the central region becomes quite stable before the disturbance reaches the clamped boundaries. Since DEPROSS 3 does not include internal damping, the plate continues to oscillate about its plastically deformed position.

In figure 3 the center deflection (taken to be the displacement of mass station 1) of a 0.091-cm- (0.036-inch-) thick L72 plate is plotted as a function of time for 1.27-cm- (0.50-inch-) diameter hail, which impacted at various velocities. The center deflection increases with time to a maximum and then oscillates elastically. Additional calculations indicate that oscillations are more pronounced for the larger hail sizes. After approximately 300 μs, plastic work ceases and the sheet has absorbed approximately 82 percent of the initial kinetic energy of the hailstone. Twelve percent of the remaining energy is elastic-strain energy, and the other 6 percent is kinetic energy. A mean value of the center deflection after 300 μs is taken as the permanent center deflection.

After long periods of computation, instabilities in some of the numerical calculations occurred. These instabilities are not easily recognized until they become pronounced. In figure 3, the computations for g_o equal to 66 m/s (216 ft/s) and 183 m/s (600 ft/s) are suspected of developing numerical instability. These instabilities were minimized by carefully choosing the time increments between calculation cycles. (See ref. 9.)

Figure 4 shows comparisons between the computer-predicted final shapes and the R.A.E. experimentally determined shapes for L72 sheets. The hailstones were 1.27 cm (0.50 inch), 2.54 cm (1 inch), and 1.91 cm (0.75 inch) in diameter (represented in the figures by their radii). There is a close correlation between the experimental data and the computer predictions; this correlation is much closer than the conical shapes predicted by the classical bending approach of reference 4. The computer predictions exhibit slightly larger overall deflections than do the experimental data and, hence, are conservative. This overprediction can be partially attributed to the neglect of strain-rate effects (see ref. 11, p. 64) in the calculations. Previous comparisons between DEPROSS 3 calculations and experimental data also indicated a slight conservatism in the calculations. (See ref. 8.) Reference 8 indicated that the specific factors responsible for this overprediction had not been isolated and resolved, but among the possible factors were an ". . . inadequate representation of the stress-strain properties of the material, neglect of strain-rate effects, an inadequate representation of the flow process, uncertainties of the externally applied forces, etc."

The lateral splash of hail on impact, observed experimentally by the R.A.E., could also contribute to this conservatism. After impact, an annulus of material from the crushed hailstone continues to move radially outward. This radial dispersion of mass is not accounted for in the DEPROSS 3 calculations. Another possible factor is the difference between the experimental sheets and computer idealization of those sheets. The experimental sheets were 20.32 cm (8 inches) square, whereas a 20.32-cm- (8-inch-) diameter circular plate was used in DEPROSS 3. The square sheet contained 27 percent more material area than the circular plate; however, this additional area was near the boundary and should have little effect on the permanent center deflection.

Permanent Center Deflection

In figures 5, 6, and 7, the computer predictions are compared with the experimentally determined permanent center deflections of L72 aluminum. The center deflections for three different sheet thicknesses are shown in each figure.

The supplementary R.A.E. data for L72 sheets impacted by 1.27-cm- (0.50-inch-) diameter hail are presented in figure 5. A solid line has been faired through the data, and the dashed line represents the theory. The theory generally overestimates the deflection. A vertical bar marked with either P or SP indicates, respectively, that the sheet was either completely penetrated or developed a split at the corresponding velocity. Supplementary data for 1.91-cm- (0.75-inch-) diameter hail are shown in figure 6. Again, the theory is generally conservative, but still closely follows the slope of the experimental data.

Figure 7 contains the data for 2.54-cm- (1-inch-) diameter hail taken from reference 5. Again, the theory is conservative but follows the slope of the experimental data.

Also shown in figure 7, by the three solid symbols, are computer results for a simply supported circular plate with the same dimensions and loading conditions as the corresponding clamped circular plates. Calculations were made for two simply supported plates: the 0.122-cm- (0.048-inch-) thick plate and the 0.091-cm- (0.036-inch-) thick plate. These results show that the boundary conditions of the plate have little effect on the permanent center deflection. These calculations for the simply supported plates also exhibited a lower frequency of elastic oscillation, as might be expected. Consequently, longer computation times were needed to establish the permanent deformations.

Comparison of Bending and Bending-Membrane Theories With Experimental Data

A comparison of the classical, thin-plate bending analysis of reference 4 and the large-deflection bending and membrane numerical analysis (DEPROSS 3) with the R.A.E. experimental data is shown in figures 8 and 9 for L72 and L73, respectively. In the figures the permanent center deflection of a 0.122-cm- (0.048-inch-) thick sheet is plotted as a function of hailstone impact velocity. Curves are presented in each figure for three different hailstone sizes, 1.27-, 1.91-, and 2.54-cm (0.50-, 0.75-, and 1-inch) diameter (represented in the figures by their radii).

The bending analysis of reference 4 was modified to include the experimentally observed spreading of the hailstone. This modification was accomplished by increasing the hailstone diameter by the factor K_2 discussed previously and decreasing the hailstone density to maintain the original mass. It was not possible to include the mass of

the hailstone after impact in the bending analysis without resorting to major modifications. The appropriate equations and the details of the calculations are contained in appendix C.

The bending-membrane theory follows the trend of the experimental data quite well, while the bending theory deviates from the data as soon as the deflection increases above the sheet thickness. The experimental data indicate a linear dependence on the hailstone velocity g_o whereas the bending theory of reference 4 yields too strong a velocity dependence, that is, $\delta \propto g_o^{2.85}$. The bending-membrane results for L72 follow the linear slope of the experimental data but are conservative. The results from the bending-membrane theory for L73 show very good agreement with the experimental data both in slope and magnitude. The better agreement with L73 data than with L72 data is probably due to a better approximation of the stress-strain behavior of L73. There may also be a strain-rate effect, but data on the effects of high strain rates on the behavior of these materials were not available.

Empirical Relationship

An attempt was made to correlate the computed center deflection curves of figures 5, 6, and 7 with one parameter. Logarithmic cross plots of the calculations were made to determine exponents, and the result of these efforts is shown in figure 10 where the center deflection is plotted as a function of $g_o a^2/h^{3/4}$ on log-log scale. The parameter reasonably correlates the curves. It is apparent that the exponent on "a" is not a constant since the curves shift as the value of "a" changes. A functional relationship more complex than "a" raised to a power is required to better correlate the curves.

CONCLUDING REMARKS

In this paper the denting process which occurs when a high-speed aircraft collides with hailstones was modeled mathematically by assuming that a crushable, spherical hailstone impacted normal to a flat sheet. The solution was accomplished by adapting the DEPROSS 3 computer program to the hail-impact problem. This analytical method considers both bending and membrane action and elastic and plastic material behavior.

The analytical results and experimental data from the British Royal Aircraft Establishment presented in this paper suggest that membrane action is a dominant factor in the denting of aircraft surfaces by hail when the deflection exceeds the sheet thickness. According to reference 4, the center deflection should vary with the hailstone velocity to the 2.85 power when membrane forces are neglected. The improved analysis of this paper, which includes membrane action, indicates that the center deflection varies with velocity to the first power.

The bending and membrane analysis of DEPROSS 3 agrees well with the experimental data for various combinations of hailstone sizes and aluminum-sheet thicknesses. Although approximate, the bilinear stress-strain relationship employed in the computer program gave results that quite closely paralleled the trend of the experimental data.

Langley Research Center,
National Aeronautics and Space Administration,
Hampton, Va., December 4, 1970.

APPENDIX A

CONVERSION OF U.S. CUSTOMARY UNITS TO SI UNITS

The International System of Units (SI) was adopted by the Eleventh General Conference on Weights and Measures, Paris, October 1960, in Resolution No. 12 (ref. 10). Conversion factors for the units used herein are given in the following table:

Physical quantity	U.S. Customary Unit	Conversion factor (a)	SI Unit
Length	in.	0.0254	meters (m)
Density	$lb\text{-}s^2/ft^4$	16.02	kilograms per cubic meter (kg/m^3)
Stress	psi (lbf/in^2)	6.895×10^3	newtons per square meter (N/m^2)
Velocity	ft/s	0.3048	meters per second (m/s)

[a]Multiply value given in U.S. Customary Unit by conversion factor to obtain equivalent value in SI Unit.

Prefixes to indicate multiple of units are as follows:

Prefix	Multiple
micro (μ)	10^{-6}
centi (c)	10^{-2}
kilo (k)	10^3
giga (G)	10^9

APPENDIX B

MODIFICATIONS TO DEPROSS 3

A listing of the velocity input section to the modified DEPROSS 3 computer program is presented in this appendix. The four subroutines PRINT, EQUIL, STRAIN, and STRESS remain essentially the same as presented in reference 9. The lack of identification numbers at the right side of the following listing indicates modifications made to the original DEPROSS 3 velocity input section.

Main Program

```
      PROGRAM DEPROS3 (INPUT,OUTPUT,TAPE5=INPUT,TAPE8)
C  CLAMPED CIRCULAR PLATE, AXISYMMETRIC MOTION (DEPROSS 3)
C  INITIAL VELOCITY DISTRIBUTION
      DIMENSION R(50),DR(50),Z(50),DZ(50),DELTS(50),DDS(50),DELTT(50),DD
     1T(50),DT(50),SINT(50),DSINT(50),COST(50),EPSITI(50),EPSITO(50),EPS
     2IPI(50),EPSIPO(50),BIGNT(50),BIGNTR(50),BIGNP(50),QTR(50),BIGMT(50
     3),BIGMP(50),RO(50),ROAVE(50),CRO(50),SINTO(50),CMASS(50),YIELD(50)
     4,ZETA(5),CZETA(5),RZETA(5,50),E(6),EPSIL(5),SIGMA(5),SNOSQ(5),HSFL
     5(5),SNT(5,5,50),SNP(5,5,50),S(50),VELOCY(50),NSTAT(50),TH(50),C5(5
     60)
      COMMON R,DR,Z,DZ,DELTS,DDS,DELTT,DDT,DT,SINT,DSINT,COST,EPSITI,EPS      0007
     1ITO,EPSIPI,EPSIPO,BIGNT,BIGNTR,BIGNP,QTR,BIGMT,BIGMP,RO,ROAVE,CRO,     0008
     2SINTO,CMASS,YIELD,ZETA,CZETA,RZETA,E,EPSIL,SIGMA,SNOSQ,HSFL,SNT,SN     0009
     3P,N,N1,N2,NFL,NSFL,NYIELD,MYIELD,KE,J,TIME,DELTSO,SNU,CINETO,HHALF     0010
     4,C2,C3,C4,C6,C7,M
 5000 CONTINUE
      READ 10,N,NFL,NSFL,M,M1,M2,KE,BIGR,H,CFL,SNU,RHO,DELTAT,D,P,(EPSIL
     1(L),SIGMA(L),L=1,NSFL)
      IF(EOF,5)400,401
  400 STOP
  401 CONTINUE
      READ  101,BIGA,RHP,GO,C10
C  MV=0 A RESTART,  MV=NEGATIVE NUMBER-STOP,  MV=POSITIVE NUMBER
C  -CALCULATES WITH INITIAL INPUT
      READ 10,MV
      REWIND 8
  101 FORMAT(4E18.8)
      PRINT 9,N,NFL,NSFL,M,M1,M2,KE,BIGR,H,CFL,SNU,RHO,DELTAT,D,P,(EPSIL
     1(L),SIGMA(L),L=1,NSFL)
    9 FORMAT(//6X1HN,4X3HNFL,3X4HNSFL,5X1HM,6X2HM1,5X2HM2,5X2HKE/717//9X
     14HBIGR,15X1HH,16X3HCFL,15X3HSNU/4E18.8//9X3HRHO,14X6HDELTAT,14X1HD
     2,17X1HP/4E18.8//8X5HEPSIL,13X5HSIGMA/(2E18.8))
      PRINT 102,BIGA,RHP,GO,C10
  102 FORMAT(//9X4HBIGA,14X3HRHP,16X2HGO,16X3HC10/(4E18.8))
   10 FORMAT(715/(4E18.8))
      PRINT 8,MV
    8 FORMAT(//4H MV=I5)
      N1= N+1                                                              0020
      N2= N                                                                0021
      NYIELD= 0                                                            0022
      DELTSO= BIGR/FLOAT(N)                                                0023
      DELT= DELTSO/2.                                                      0024
```

```
      FLONFL= NFL                                                          0025
      HFL= H/FLONFL                                                        0026
      HHALF= H/2.                                                          0027
      DHALF= HHALF/SQRT(FLONFL**2-CFL)                                     0028
      E(1)= SIGMA(1)/EPSIL(1)                                              0029
      C1= E(1)/(1.-SNU**2)                                                 0030
      C2= C1/DELTS0                                                        0031
      C3= -2.*SNU                                                          0032
      C4= 3.141592653590*DELTS0/E(1)                                       0033
      DELTAR= BIGR/FLOAT(N)
      R1= DELTAR/2.
      LOAD= BIGA/DELTAR
      MOAD= LOAD-1
      IF(BIGA.GT.BIGR) MOAD=N
      STH= 0.
     † C9=2./((C10**3-(C10**2-1.)**1.5)*C10**2)
      IF(MOAD.LE.0) GO TO 3
      DO  3 NV=1,MOAD
      S(NV)= (2.*FLOAT(NV)-1.)*R1
      TH(NV)= C9*SQRT(BIGA**2-S(NV)**2)
      STH= (2.*FLOAT(NV)-1.)*TH(NV)+STH
      NSTAT(NV)= NV
    3 CONTINUE
      IF(BIGA.GT.BIGR) GO TO 4
      NV= LOAD
      IF(NV.EQ.0)NV=1
      S(NV)= (2.*FLOAT(NV)-1.)*R1
      TH(NV)= BIGA**3*1./3.*C9/(2.*R1**2*(2.*FLOAT(NV)-1.))-STH/(2.*FLOA
     1T(NV)-1.)
      NSTAT(NV)= NV
    4 CONTINUE
      L1= LOAD
      IF(BIGA.GT.BIGR) L1= N
      PRINT 104,(NSTAT(NV),TH(NV),NV=1,L1)
  104 FORMAT(//3X5HNSTAT,9X2HTH/(I6,E18.6))
      DO 5 I=1,LOAD
      C5(I)= DELTAT**2/(RHO*H*DELTS0+RHP*TH(I)*DELTS0)
    5 CONTINUE
      NOAD= LOAD+1
      DO 6 I=NOAD,N1
      C5(I)= DELTAT**2/(RHO*H*DELTS0)
    6 CONTINUE
      IF(D)210,12,11                                                       0035
   11 C6= 1./P                                                             0036
      C7= 1.1547005/D/DELTAT/C1                                            0037
      GO TO 13                                                             0038
   12 C6= 1.                                                               0039
      C7= 0.                                                               0040
   13 IF(NSFL-1)210,16,14                                                  0041
   14 DO 15 L=2,NSFL                                                       0042
      E(L)= (SIGMA(L)-SIGMA(L-1))/(EPSIL(L)-EPSIL(L-1))                    0043
   15 CONTINUE                                                             0044
   16 E(NSFL+1)= 0.                                                        0045
      DO 17 L=1,NSFL                                                       0046
      HSFL(L)= HFL*(E(L)-E(L+1))/E(1)                                      0047
      SNOSQ(L)= (E(1)*EPSIL(L))**2                                         0048
   17 CONTINUE                                                             0049
      NFL1= NFL/2                                                          0050
      DO 20 K=1,NFL1                                                       0051
```

†$C_9 = K_1$ (see eq. (1)).

```
      L= NFL-K+1                                                        0052
      ZETA(K)= DHALF*FLOAT(L-K)                                         0053
      ZETA(L)= -ZETA(K)                                                 0054
      CZETA(K)= C2*ZETA(L)                                              0055
   20 CZETA(L)= -CZETA(K)                                               0056
      DO 21 I=1,N1                                                      0057
      SINTO(I)= 0.                                                      0058
      RO(I)= DELT*FLOAT(I+I-1)                                          0059
      CRO(I)= C1/RO(I)                                                  0060
      CMASS(I)= C5(I)/RO(I)
   21 CONTINUE                                                          0062
      DO 23 I=2,N1                                                      0063
      ROAVE(I)=(RO(I)+RO(I-1))/2.                                       0064
      C1R=-C1/ROAVE(I)                                                  0065
      DO 22 K=1,NFL                                                     0066
      RZETA(K,I)=C1R*ZETA(K)                                            0067
   22 CONTINUE                                                          0068
   23 CONTINUE                                                          0069
      IF(MV)210,90,30                                                   0070
   30 MYIELD= 0                                                         0071
      J= 0                                                              0072
      TIME= 0.                                                          0073
      DO 50 I=1,N1                                                      0074
      R(I)= RO(I)                                                       0075
      DR(I)= 0.                                                         0076
      Z(I)= 0.                                                          0077
      DZ(I)= 0.                                                         0078
      DELTS(I)= DELTSO                                                  0079
      DELTT(I)= 0.                                                      0080
      SINT(I)= 0.                                                       0081
      COST(I)= 1.                                                       0082
      BIGNT(I)= 0.                                                      0083
      BIGNP(I)= 0.                                                      0084
      BIGMT(I)= 0.                                                      0085
      BIGMP(I)= 0.                                                      0086
      YIELD(I)= 55555555000000000008                                    0087
      DO 40 K=1,NFL                                                     0088
      DO 39 L=1,NSFL                                                    0089
      SNT(L,K,I)= 0.                                                    0090
      SNP(L,K,I)= 0.                                                    0091
   39 CONTINUE                                                          0092
   40 CONTINUE                                                          0093
   50 CONTINUE                                                          0094
      C1= C9*BIGA/H*RHP/RHO
      DELTAR= BIGR/FLOAT(N)
      R1= DELTAR/2.
      LOAD= BIGA/DELTAR
      MOAD= LOAD-1
      IF(BIGA.GT.BIGR) MOAD=N
      SZDOTO= 0.
      IF(MOAD.LE.0) GO TO 80
      DO 80 NV=1,MOAD
      S(NV)= (2.*FLOAT(NV)-1.)*R1
      VELOCY(NV)= C1*GO*SQRT(BIGA**2-S(NV)**2)/(BIGA+C1*SQRT(BIGA**2-S(N
     1V)**2))
      SZDOTO= (2.*FLOAT(NV)-1.)*VELOCY(NV)+SZDOTO
      ZDOTO= VELOCY(NV)
      I1= NV
      I2= NV
      NSTAT(NV)= NV
      DELTAZ= DELTAT*ZDOTO                                              0100
      DO 70 I=I1,I2                                                     0101
      DZ(I)= DELTAZ                                                     0102
```

```
 70 CONTINUE                                                                    0103
 80 CONTINUE                                                                    0104
    IF(BIGA.GT.BIGR) GO TO 86
    NV= LOAD
    IF(NV.EQ.0)NV=1
    S(NV)= (2.*FLOAT(NV)-1.)*R1
    VELOCY(NV)= BIGA**2*GO*(.5-1./C1+1./C1**2*ALOG(1.+C1))/(2.*R1**2*(
   12.*FLOAT(NV)-1.))-(SZDOTO/(2.*FLOAT(NV)-1.))
    ZDOTO= VELOCY(NV)
    I1= NV
    I2= NV
    NSTAT(NV)= NV
    DELTAZ= DELTAT*ZDOTO
    DO 85 I=I1,I2
    DZ(I)= DELTAZ
 85 CONTINUE
 86 DZ(N)= 0.                                                                   0105
    L1= LOAD
    IF(BIGA.GT.BIGR) L1= N
    PRINT 103,(NSTAT(NV),S(NV),VELOCY(NV),NV=1,L1)
103 FORMAT(//3X5HNSTAT,9X1HS,15X6HVELOCY/(I6,2E18.6))
    CALL PRINT                                                                  0106
    GO TO 110                                                                   0107
 90 READ TAPE 8,J,MYIELD, CINETO,(R(I),DR(I),Z(I),DZ(I),DELTS(I),DELTT          0108
   1(I),SINT(I),COST(I),((SNT(L,K,I), SNP(L,K,I),L=1,NSFL),K=1,NFL),I=          0109
   21,N1),TIME,(BIGNT(I),BIGNP(I),BIGMT(I),BIGMP(I),YIELD(I),I=1,N)
    CALL PRINT
    REWIND 8
110 BIGNTR(1)= 0.                                                               0111
    QTR(1)= 0.                                                                  0112
    DT(1)= 0.                                                                   0113
    QTR(N+1)= 0.                                                                0114
    DT(N+1)= 0.                                                                 0115
    DSINT(N+1)= 0.                                                              0116
    DDT(N+1)= 0.                                                                0117
120 J= J+1                                                                      0118
    DDS(1)= 2.*DR(1)                                                            0119
    DDS(N+1)= (-2.)*DR(N)                                                       0120
    CALL STRAIN                                                                 0121
    CALL STRESS                                                                 0122
    CALL EQUILI                                                                 0123
    DZ(N)=0.
    IF(J-M1)130,140,210                                                         0124
130 IF(NYIELD)150,160,150                                                       0125
140 M1= M1+M2                                                                   0126
150 TIME= DELTAT*FLOAT(J)                                                       0127
    CALL PRINT                                                                  0128
    NYIELD= 0
160 IF(J-M)120,170,210                                                          0130
170 IF(MYIELD)180,200,180                                                       0131
180 TIME= DELTAT*FLOAT(MYIELD)                                                  0132
    PRINT 190,TIME                                                              0133
190 FORMAT(28H0     FIRST YIELDING AT TIME=E12.5)                               0134
200 WRITE TAPE8,J,MYIELD, CINETO,(R(I),DR(I),Z(I),DZ(I),DELTS(I),DELTT          0135
   1(I),SINT(I),COST(I),((SNT(L,K,I), SNP(L,K,I),L=1,NSFL),K=1,NFL),I=          0136
   21,N1),TIME,(BIGNT(I),BIGNP(I),BIGMT(I),BIGMP(I),YIELD(I),I=1,N)
210 GO TO 5000
    END                                                                         0139
```

Input Data

The following data are input for a typical computer run for the clamped, 8-inch-diameter, circular plate. This particular run is for $a = 0.5$ inch, $K_2 = 1.5$, $g_o = 1279$ ft/sec, and $h = 0.036$ inch. The input to DEPROSS 3, as described in reference 9, is given in the in-lb-sec system; therefore, the input data presented in this appendix are given only in the in-lb-s system.

The input data (see ref. 9) are as follows:

N = 32	number of mass points along the radius of sheet
NFL = 4	number of layers specifying the sheet thickness
NSFL = 2	number of sublayers in strain-hardening model = number of coordinate pairs of stress and strain (i.e., 2) defining bilinear stress-strain curve
M = 18 000	cycle at which run is to stop
M1 = 200	cycle at which regular printing is to begin
M2 = 200	print every M2 cycles
KE = 0	strains on the surfaces of the sheet are omitted in print sequence
= 1	strains on the surfaces of the sheet are printed
BIGR = 4.0 in.	radius of circular sheet, b
H = 0.036 in.	thickness of sheet
CFL = 0.	layered cross section equivalent to fully plastic cross section
= 1.	layered cross section equivalent to fully elastic cross section
SNU = 1/3	Poisson's ratio
RHO = 2.62012×10^{-4} lb-sec^2/in^4	mass density of sheet material
DELTAT = 0.3×10^{-7} sec	time interval per cycle
D, P = 0.	pertain to constants used in strain-rate formula (see ref. 9) which were neglected in present application of DEPROSS 3

EPSIL (1) = 0.003627	strain at yield stress
SIGMA (1) = 38080 lb/in^2	stress at yield
EPSIL (2) = 0.15	strain (approximate) at ultimate stress
SIGMA (2) = 64064 lb/in^2	stress at ultimate strain
BIGA = 0.75 in.	radius of crushed hailstone, A
RHP = 0.80704143 × 10^{-4} lb-sec^2/in^4	mass density of hail (ice)
GO = 15348 in./sec	hailstone velocity prior to impact
C10 = 1.5	multiplication factor related to the instantaneous spread of the hailstone base at impact, K_2
MV	program instruction
1	indicates an initial computer run and the velocity distribution is calculated by the program
0	indicates a restart and the velocity distribution is read off a tape

The input data appear on the data cards as

```
32     4     230000   200   200
     .40000000+1        .36000000-1        0.                    .33333333+0
     .26201200-3        .3         -7
     .36270000-2        .3808      +5      .15000000+0           .64064     +5
     .75        +0      .80704143-4        .15348000+5           .15000000+1
 1
```

APPENDIX C

CLASSICAL THIN-PLATE BENDING ANALYSIS

Determination of Radius of Central Plastic Region

In reference 4 an elastic analysis was used to determine the radial and circumferential bending-moment distributions in an infinite sheet impacted by a hailstone. The area of the sheet around the center of impact, where the moments exceed the elastic yield moment, was determined from the moment distributions of the elastic analysis. This central plastic region was then approximated by a simply supported plastic plate. A rigid-plastic analysis applied to this plastic plate determined the permanent deformation or dent.

The simple-support boundary conditions of the rigid-plastic analysis are $M_r = 0$ and $M_\theta = M_o$. Hence, the periphery of the central plastic region was taken to be at the radius ξ where $M_r = 0$ and $M_\theta = M_o$, simultaneously. This radius was determined in the following manner: By setting $M_r(\eta,\tau)$ equal to zero in equation (11) of reference 4

$$M_r(\eta,\tau) = -\frac{DkV_o\sqrt{\frac{\pi}{2}}}{6A^2}\int_0^\infty J_{3/2}(p)\sin(p^2\tau)p^{-1/2}\left\{3\left[J_2(p\eta) - J_0(p\eta)\right] - \frac{2}{\eta}p^{-1}J_1(p\eta)\right\}dp = 0 \quad (C1)$$

specific values of the nondimensional radial location η can be determined for various values of the nondimensional time parameter τ. With these specific values of $\eta = \xi$ and τ and M_θ equated to M_o in equation (12) of reference 4

$$M_\theta = -\frac{DkV_o\sqrt{\frac{\pi}{2}}}{6A^2}\int_0^\infty J_{3/2}(p)\sin(p^2\tau)p^{-1/2}\left[-\frac{6}{\eta}p^{-1}J_1(p\eta) + J_2(p\eta) - J_0(p\eta)\right]dp = M_o \quad (C2)$$

corresponding values of hailstone velocity $\left(V_o \text{ or } g_o\right)$ can be determined for particular sheet and hailstone properties of interest.

In figures 11 and 12, respectively, the dimensionless radius of the plastic region ξ is plotted as a function of hailstone velocity g_o for a 0.122-cm- (0.048-inch-) thick L72 and L73 aluminum sheet. A curve is given in each figure for the 1.27-, 1.91-, and 2.54-cm- (0.5-, 0.75-, and 1-inch-) diameter hailstones (represented in the figures by their radii). In the calculation of these curves, the hailstone radii were increased by the appropriate K_2 factor to account for the experimentally observed spreading discussed

previously. The radius of the plastic region and other pertinent sheet and hailstone parameters can now be used to determine the permanent deformation or dent.

Determination of Permanent Center Deformation

The permanent center deflection δ of the plastically deformed plate can be determined from the following equation (see eq. (16) of ref. 4):

$$\delta = \frac{\mu V_o^2 A^2 \xi^2}{12 M_o}\left[-\frac{1}{2} + \frac{4}{\xi^2} + \sqrt{1 - \left(\frac{1}{\xi}\right)^2}\left(1 - \frac{3}{\xi^2} + \frac{1}{2\xi^4}\right) - \frac{3}{2\xi^3}\sin^{-1}\left(\frac{1}{\xi}\right)\right] \qquad (1 \leqq \xi \leqq \infty)$$

$$\delta = \frac{\mu V_o^2 A^2 \xi^2}{12 M_o}\left[-\frac{1}{2} + \frac{4}{\xi^2} + \sqrt{1 - \xi^2}\left(1 - \frac{5}{2\xi^2}\right) - \frac{3}{2\xi^3}\sin^{-1}(\xi)\right] \qquad (\xi \leqq 1) \qquad \text{(C3)}$$

with the appropriate values of A, μ, h, M_o, ρ_s, ρ_p, g_o, and V_o, where

$$V_o = \frac{\frac{2A}{h}\frac{\rho_p}{\rho_s} g_o}{1 + \frac{2A}{h}\frac{\rho_p}{\rho_s}\psi} \qquad \text{(C4)}$$

and $\psi = 0.70$.

REFERENCES

1. Roys, George P.: Airborne Instrumentation System for Measuring Meteorological Phenomena Inside Thunderstorms. ASD-TDR-63-231, U.S. Air Force, May 1963.

2. Williamson, R. E.: Aircraft Probing of Hailstorms. MRI69 FR-841 (NSF Grant GA-935), Meteorology Research, Inc., Jan. 14, 1969.

3. Souter, Robert K.; and Emerson, Joseph B.: Summary of Available Hail Literature and the Effect of Hail on Aircraft in Flight. NACA TN 2734, 1952.

4. Thomson, Robert G.; and Hayduk, Robert J.: An Analytical Evaluation of the Denting of Airplane Surfaces by Hail. NASA TN D-5363, 1969.

5. McNaughtan, I. I.; and Chisman, S. W.: A Study of Hail Impact at High Speed on Light Alloy Plates. Proceedings of the Ninth Annual National Conference on Environmental Effects on Aircraft and Propulsion Systems. Nav. Air Propulsion Test Center, 1969, pp. 16-1-16-7.

6. Florence, A. L.: Circular Plate Under a Uniformly Distributed Impulse. Int. J. Solids Struct., vol. 2, no. 1, Jan. 1966, pp. 37-46.

7. Leech, John W.; Pian, T. H. H.; Witmer, Emmett A.; and Herrmann, Walter: Dynamic Response of Shells to Externally-Applied Dynamic Loads. ASD-TDR-62-610, U.S. Air Force, Nov. 1962. (Available from DDC as AD 294 384.)

8. Witmer, Emmett A.; Balmer, Hans A.; Leech, John W.; and Pian, Theodore H. H.: Large Dynamic Deformations of Beams, Rings, Plates, and Shells. AIAA J., vol. 1, no. 8, Aug. 1963, pp. 1848-1857.

9. Balmer, Hans A.: Computer Programs to Calculate the Dynamic Elastic-Plastic Axisymmetric Responses of Impulsively-Loaded Circular Plates and Shells of Revolution. ASRL TR 128-2, Massachusetts Inst. Technol., Dec. 1964.

10. Comm. on Metric Pract.: ASTM Metric Practice Guide. NBS Handbook 102, U.S. Dep. Com., Mar. 10, 1967.

11. Witmer, E. A.; Clark, E. N.; and Balmer, H. A.: Experimental and Theoretical Studies of Explosive-Induced Large Dynamic and Permanent Deformations of Simple Structures. Exp. Mech., vol. 7, Feb. 1967, pp. 56-66.

TABLE I.- MATERIAL PROPERTIES[a]

Material	Yield stress		Yield strain	Ultimate stress		Ultimate strain	Density		Modulus of elasticity	
	psi	MN/m^2		psi	MN/m^2		$lb\text{-}s^2/in^4$	kg/m^3	psi	GN/m^2
L72 (2014-T4)	38 000	262	3.63×10^{-3}	64 000	441.3	0.150	2.62×10^{-4}	2800	10.5×10^6	72.4
L73 (2014-T6)	58 250	401.6	5.55×10^{-3}	67 000	462	.090	2.62×10^{-4}	2800	10.5×10^6	72.4
Ice							$.81 \times 10^{-4}$	866		

[a]The input to DEPROSS 3, as described in reference 9, is given in the in-lb-s system.

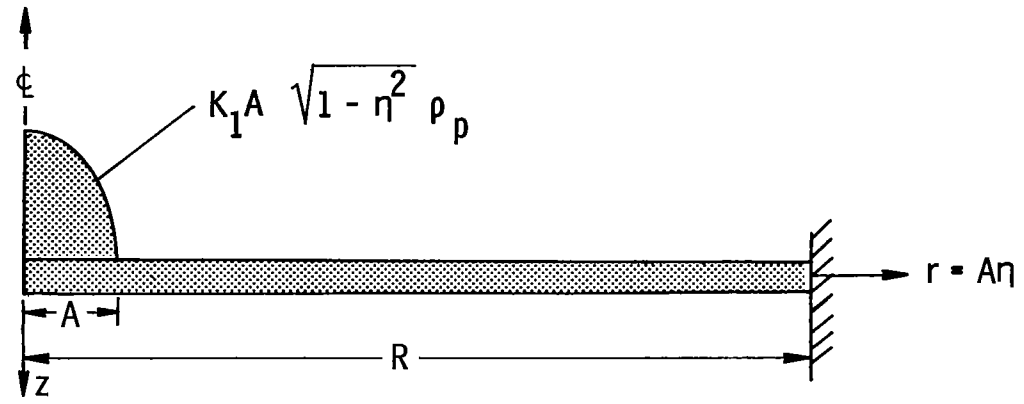

(a) Mass distribution of clamped plate and crushed hailstone.

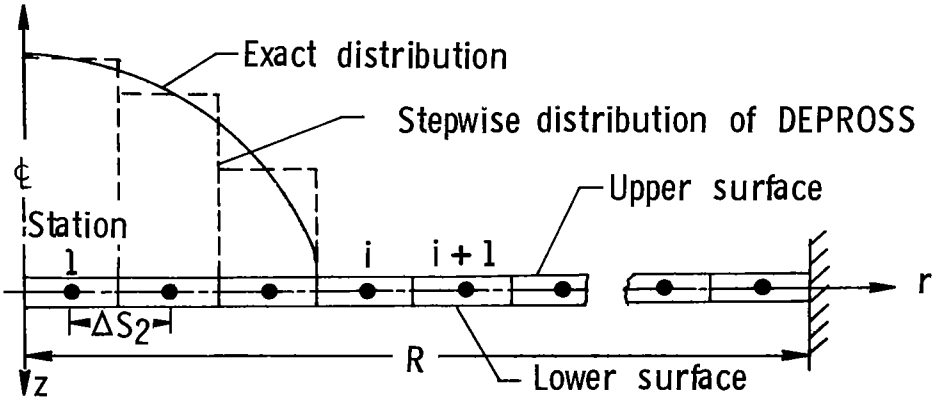

(b) Velocity and/or mass distribution approximations used in DEPROSS.

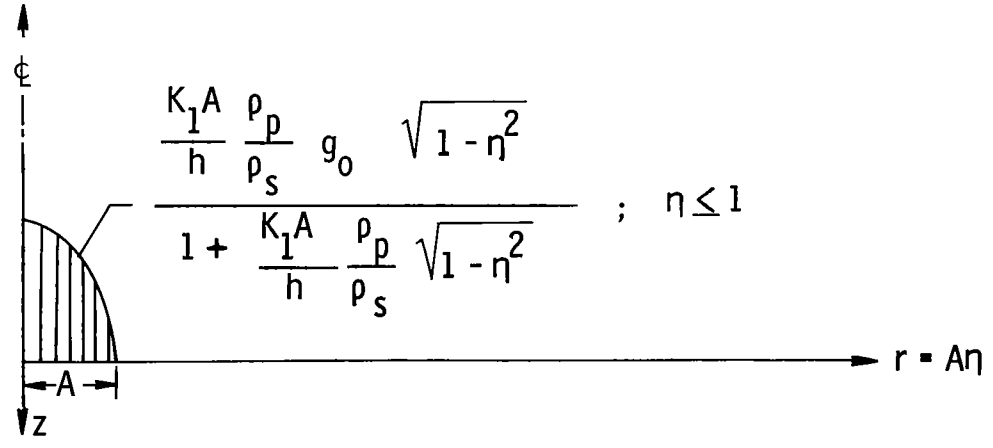

(c) Initial velocity distribution of clamped plate and crushed hailstone.

Figure 1.- Mass distribution, velocity and/or mass distribution approximations, and initial velocity distribution for a clamped circular plate impacted by a hailstone.

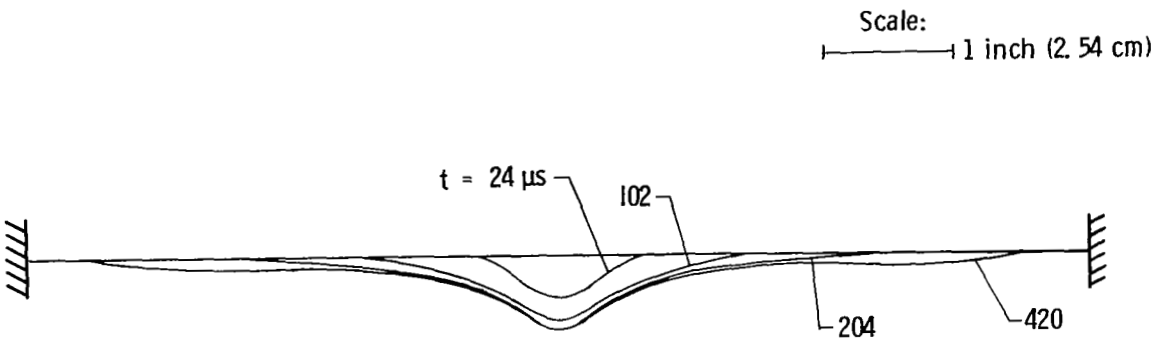

(a) Normal impact; a = 0.635 cm (0.25 inch); g_o = 658 m/s (2160 ft/s); h = 0.091 cm (0.036 inch).

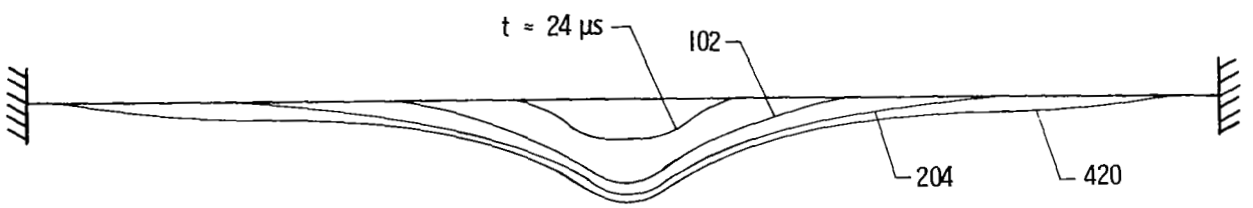

(b) Normal impact; a = 0.952 cm (0.375 inch); g_o = 547.1 m/s (1795 ft/s); h = 0.122 cm (0.048 inch).

Figure 2.- Computed shapes at different times for two specific hail impacts. (Deformations to scale.)

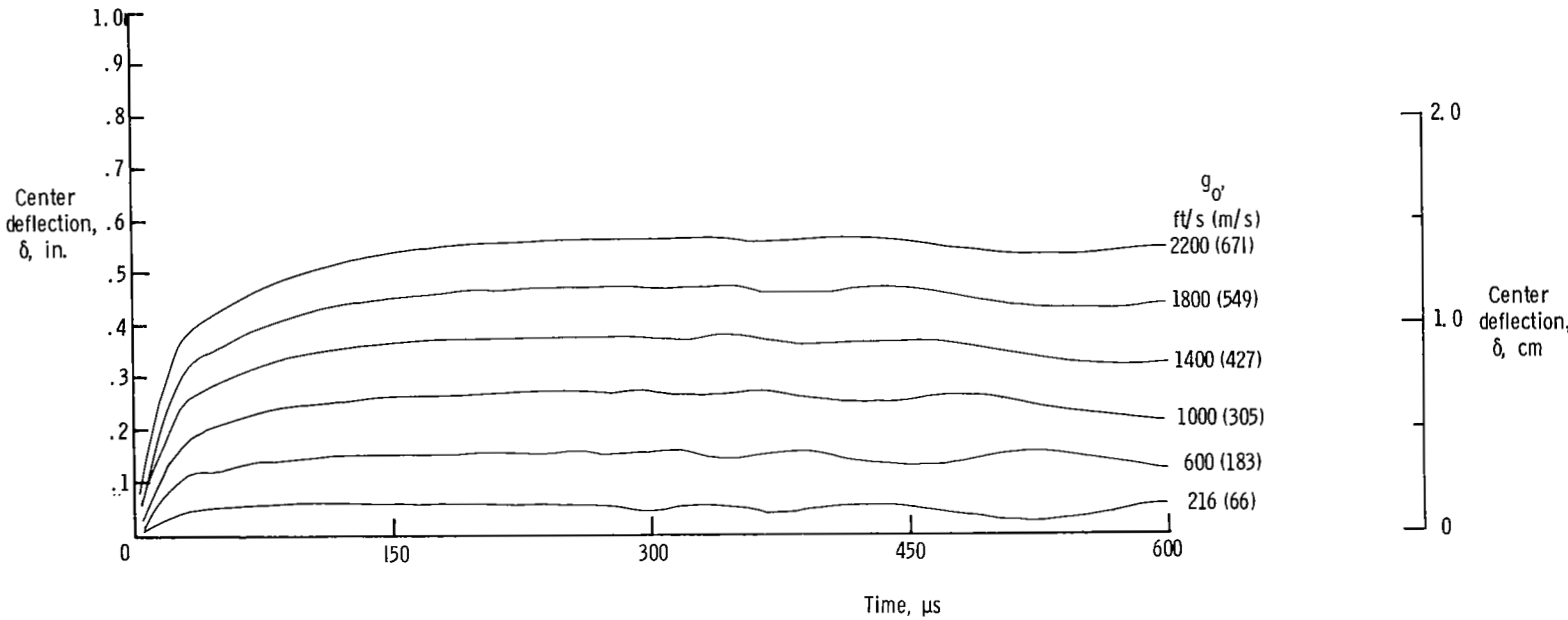

Figure 3.- Center deflection as a function of time for a 1.27-cm- (0.50-inch-) diameter hailstone impacting a 0.091-cm- (0.036-inch-) thick L72 aluminum sheet at various velocities.

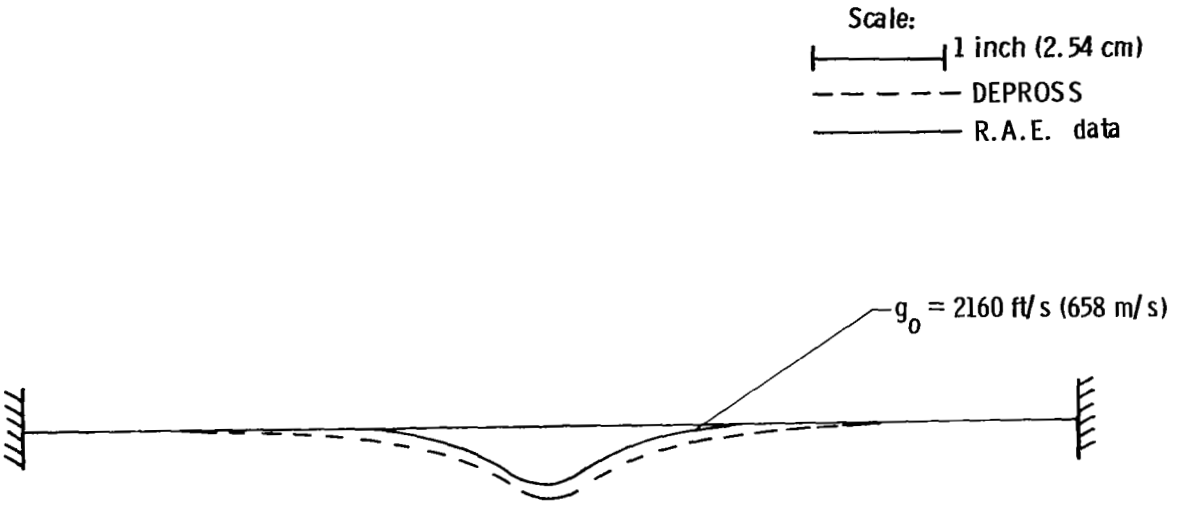

(a) Normal impact; a = 0.635 cm (0.25 inch); h = 0.091 cm (0.036 inch).

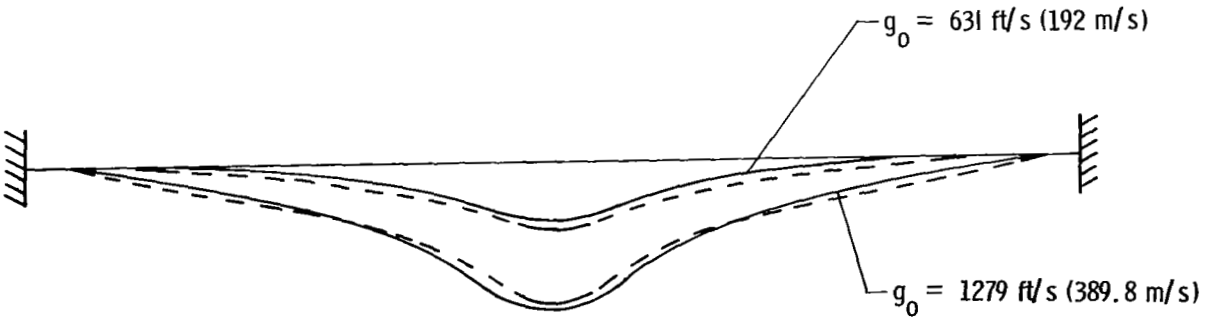

(b) Normal impact; a = 1.27 cm (0.50 inch); h = 0.091 cm (0.036 inch).

Figure 4.- Comparison of theoretical and experimental sheet deflections for L72 aluminum. (Deformations to scale.)

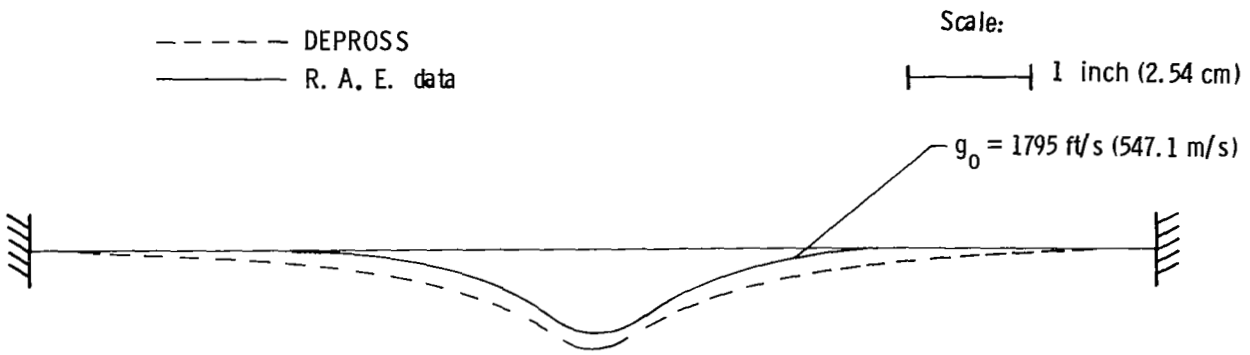

(c) Normal impact; a = 0.952 cm (0.375 inch); h = 0.122 cm (0.048 inch).

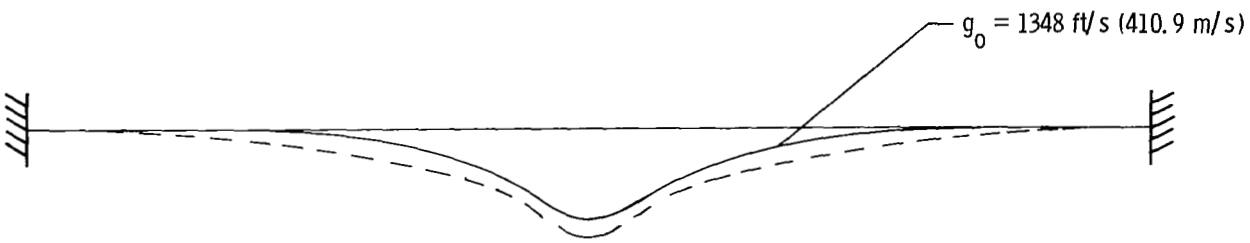

(d) Normal impact; a = 0.952 cm (0.375 inch); h = 0.071 cm (0.028 inch).

Figure 4.- Concluded.

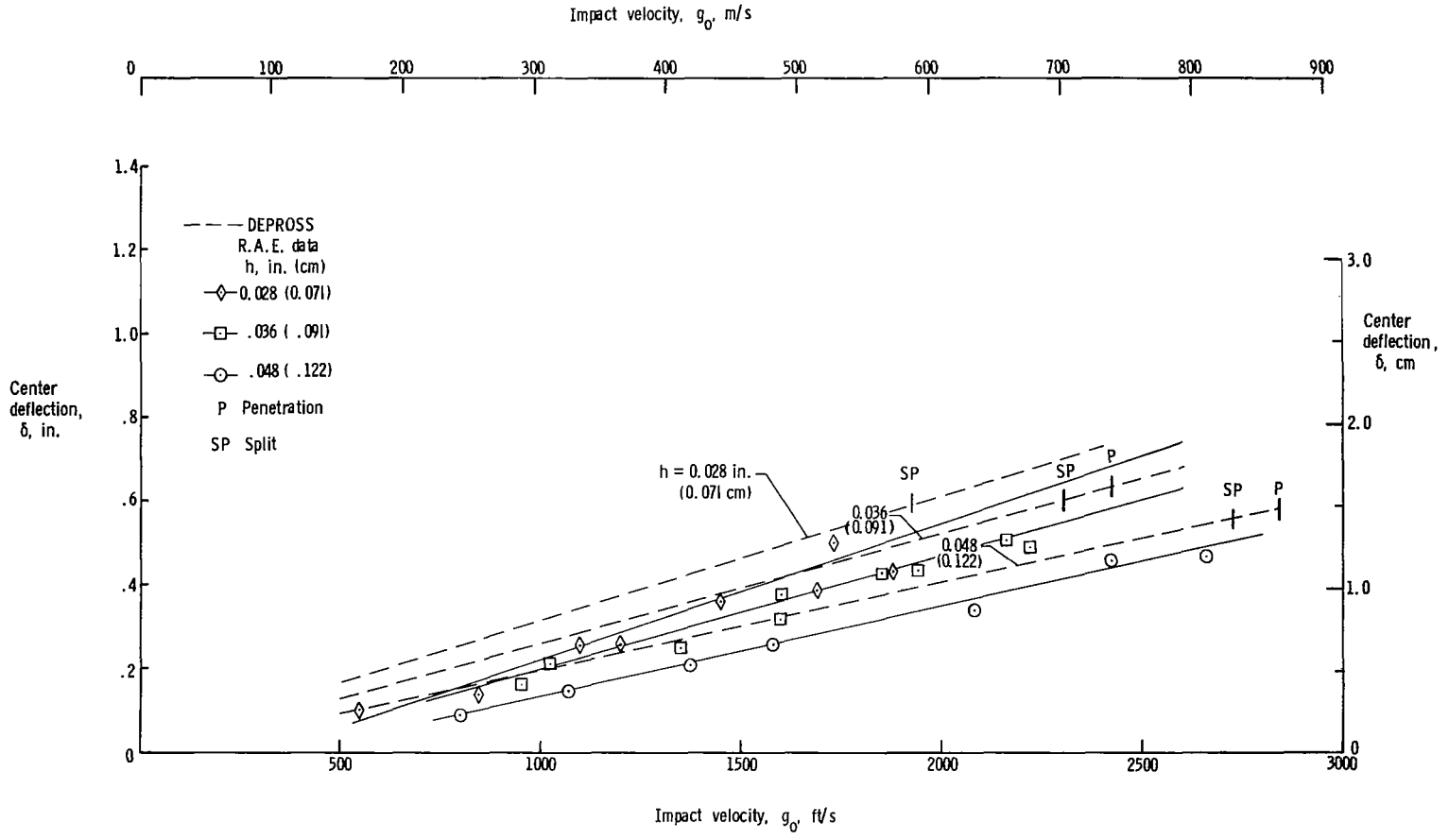

Figure 5.- Comparison of theoretical and experimental center deflections of L72 aluminum sheets impacted by 1.27-cm- (0.50-inch-) diameter hailstones.

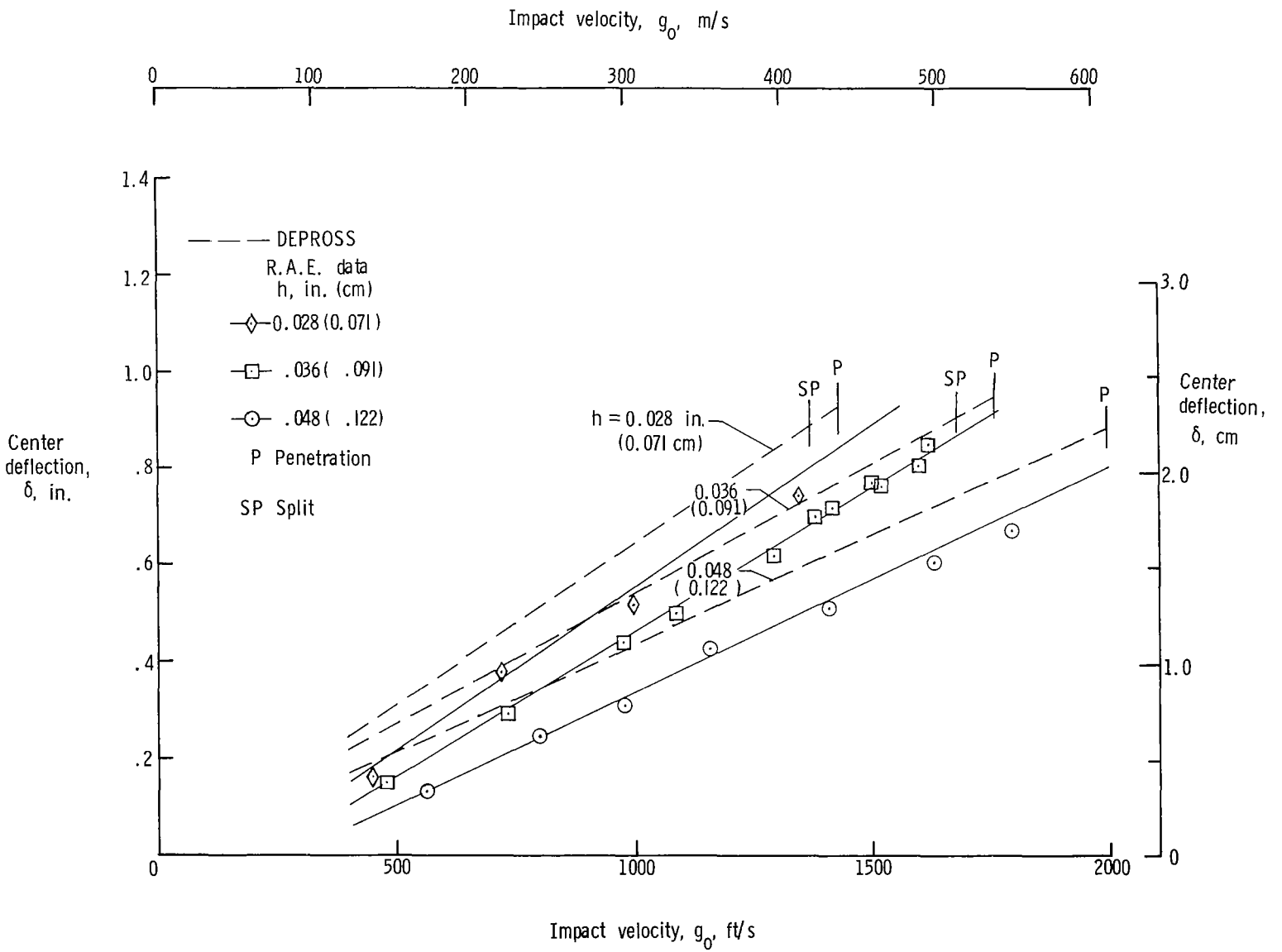

Figure 6.- Comparison of theoretical and experimental center deflections of L72 aluminum sheets impacted by 1.91-cm- (0.75-inch-) diameter hailstones.

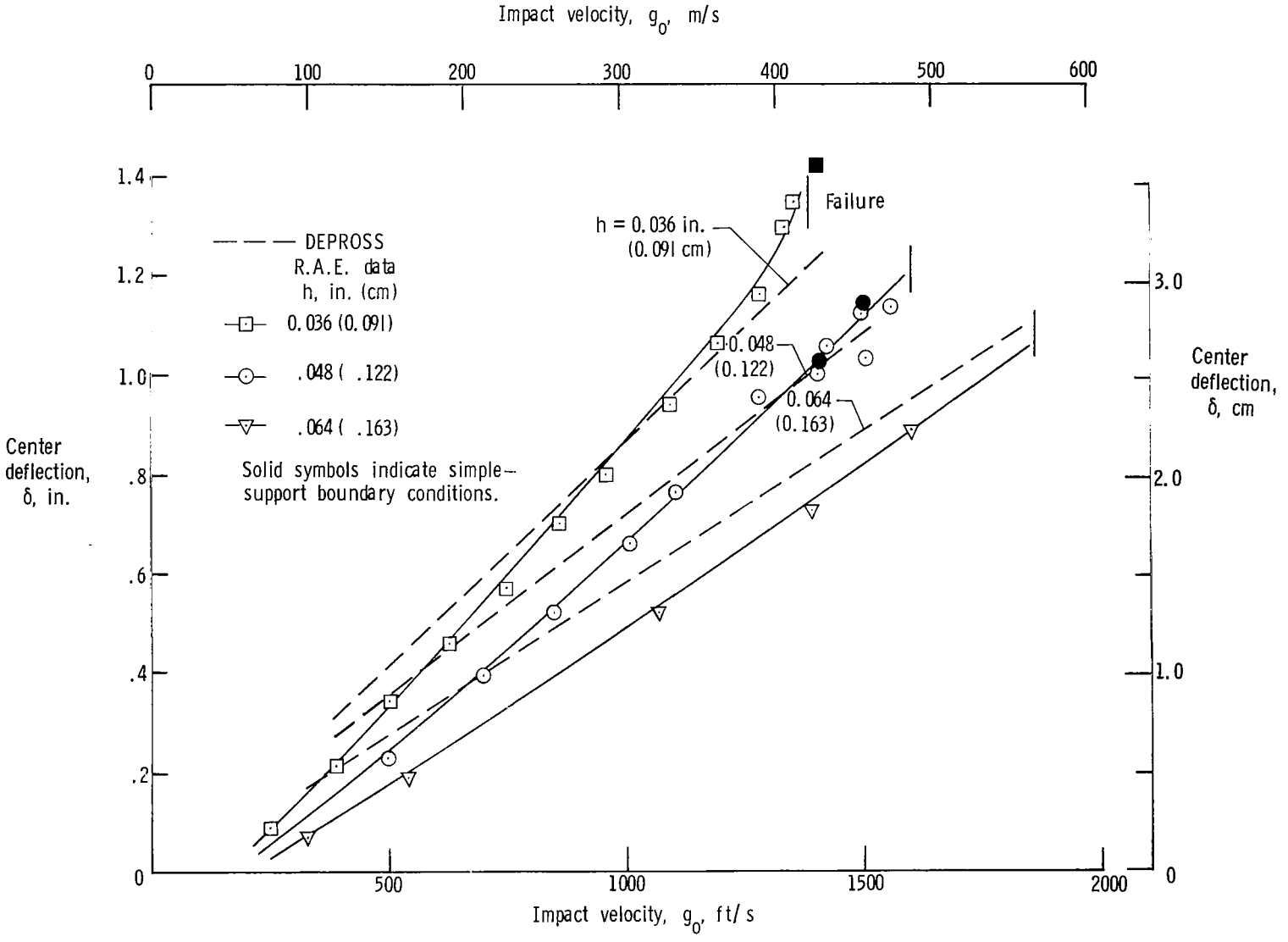

Figure 7.- Comparison of theoretical and experimental center deflections of L72 aluminum sheets impacted by 2.54-cm- (1-inch-) diameter hailstones.

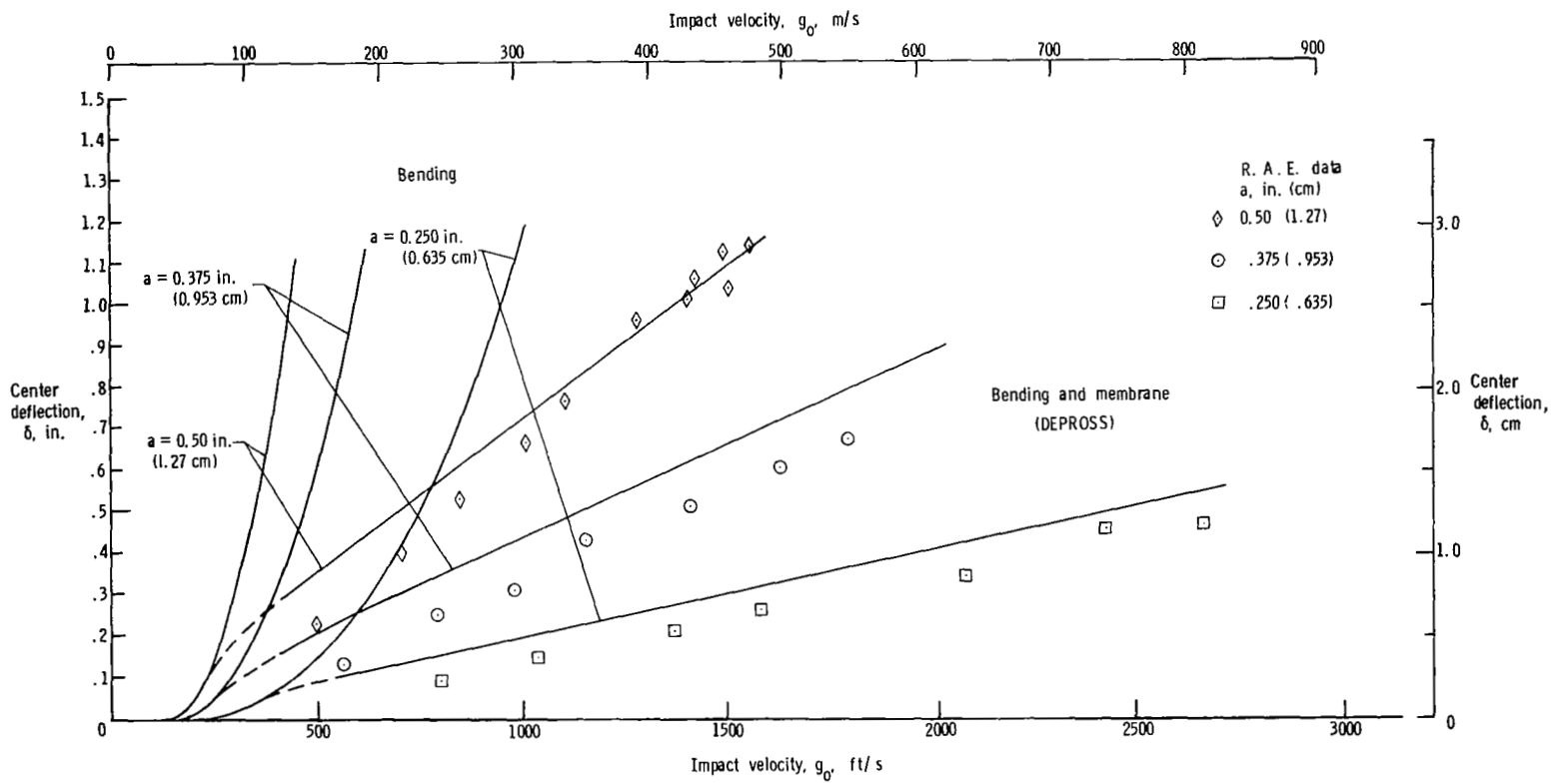

Figure 8.- Comparison of bending and bending-membrane theory with experimental data for 0.122-cm- (0.48-inch-) thick L72 aluminum sheet.

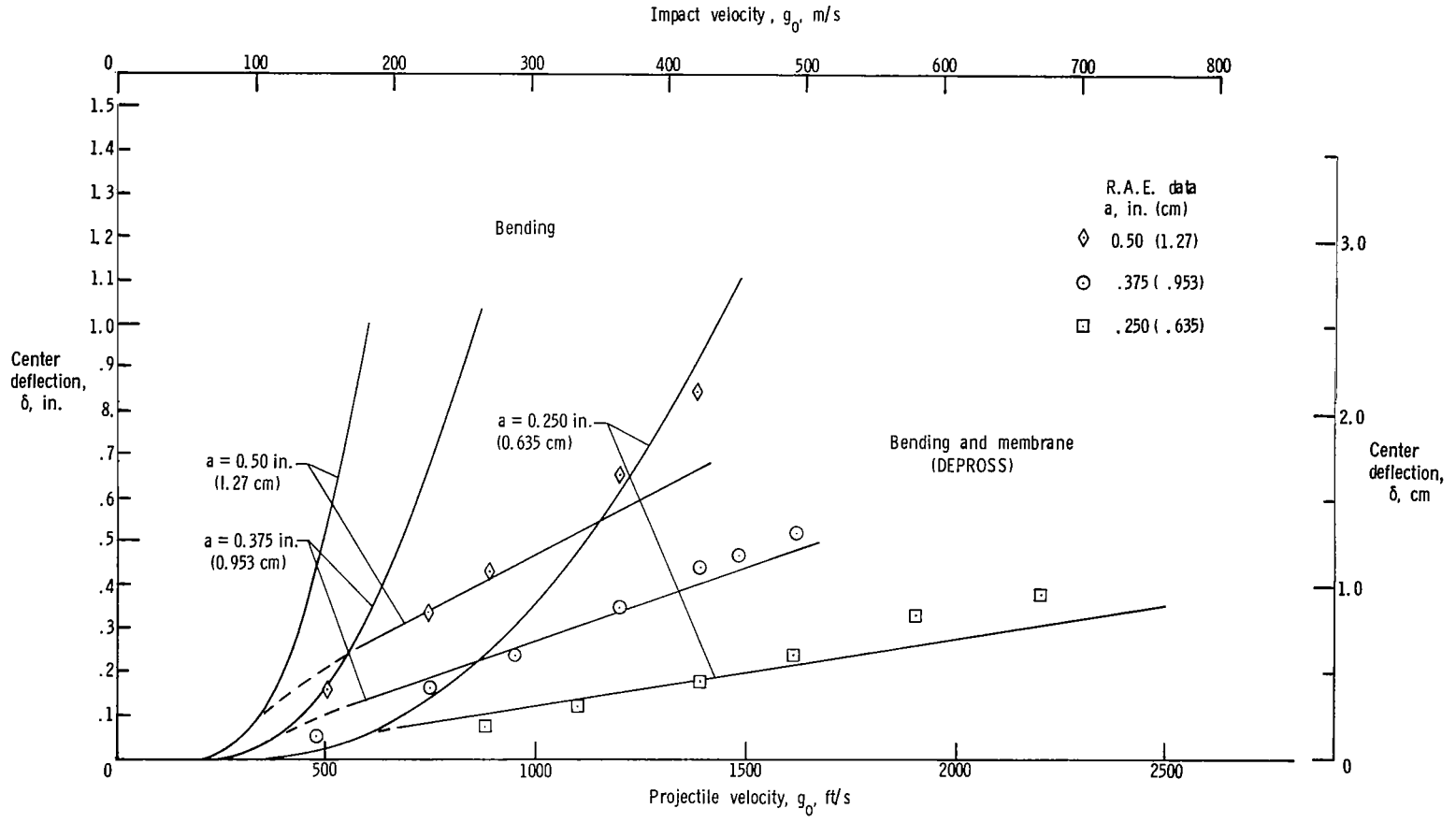

Figure 9.- Comparison of bending and bending-membrane theory with experimental data for 0.122-cm- (0.048-inch-) thick L73 aluminum sheet.

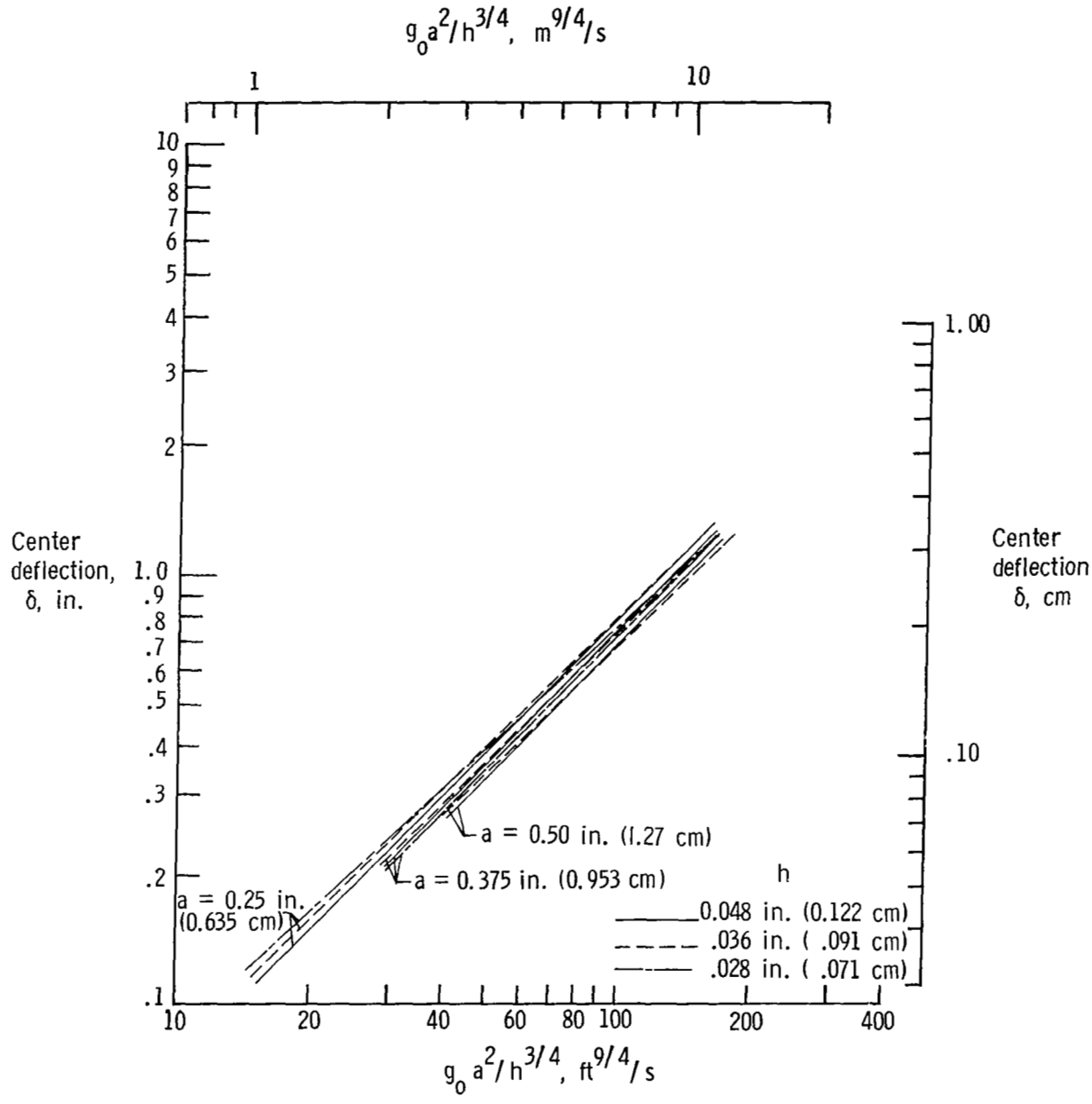

Figure 10.- Center deflection δ as a function of $g_o a^2/h^{3/4}$.

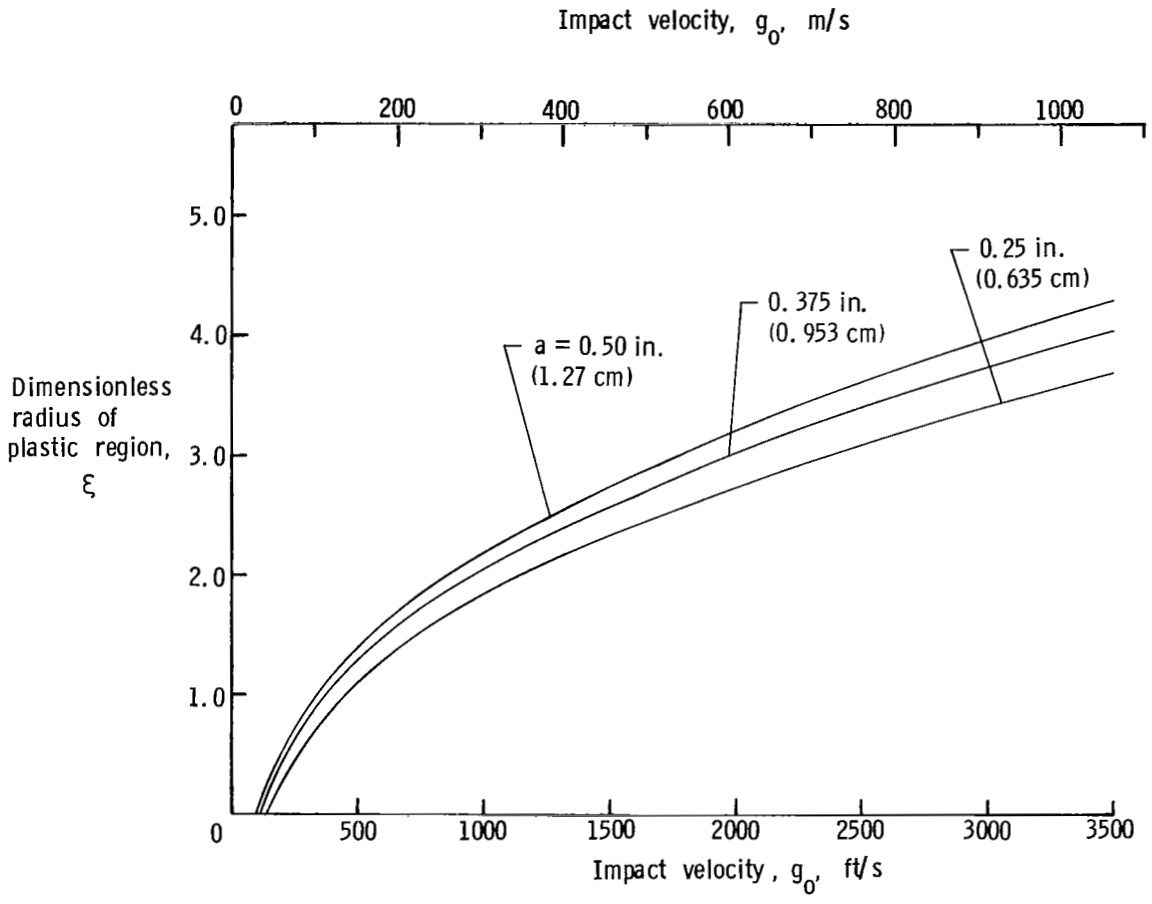

Figure 11.- Radius of plastic region as a function of hailstone velocity for aluminum alloy L72. h = 0.122 cm (0.048 inch).

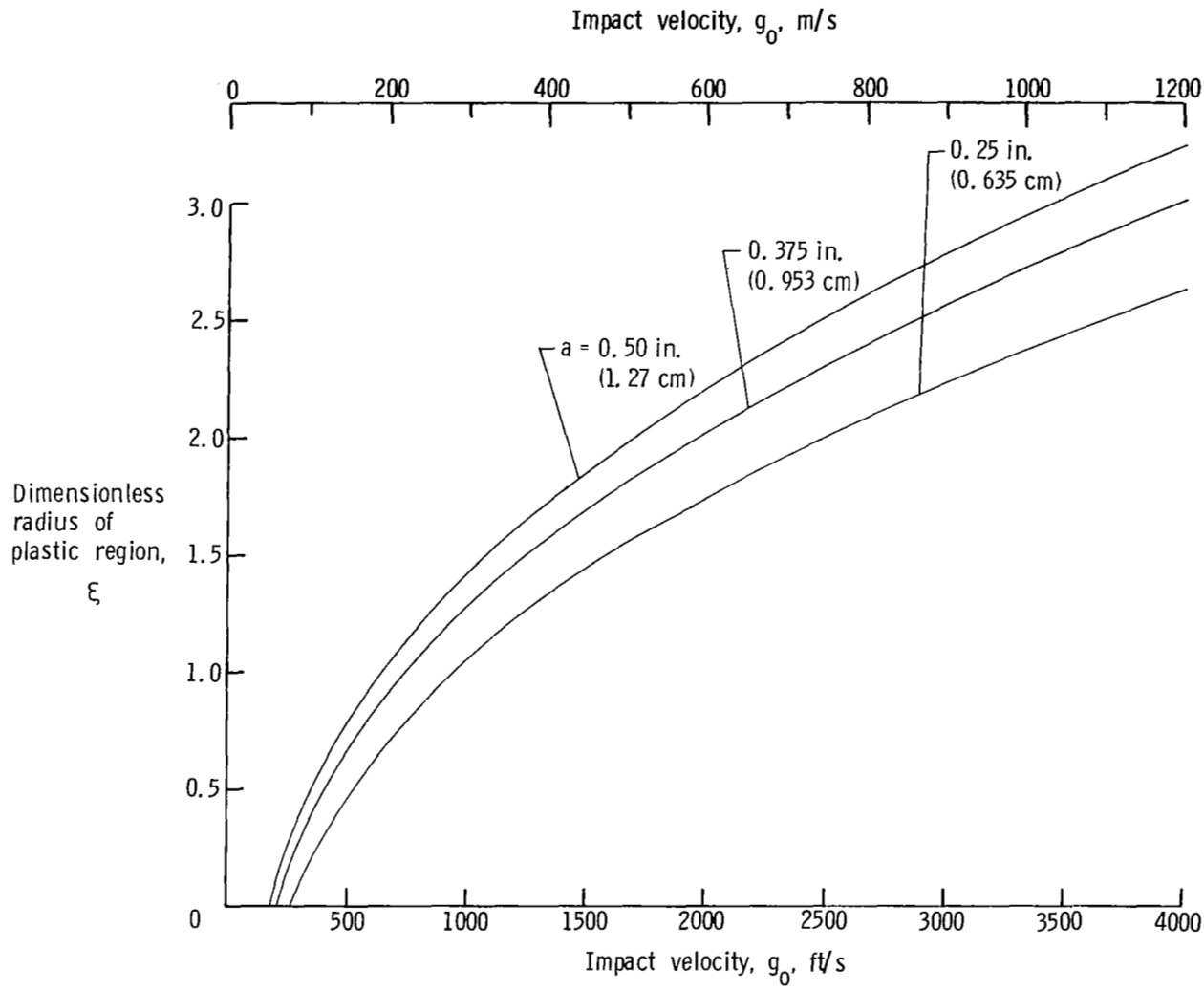

Figure 12.- Radius of plastic region as a function of hailstone velocity for aluminum alloy L73. h = 0.122 cm (0.048 inch).

NASA-Langley, 1971 —— 32 L-7343